ChemPhysChem

Research Article
doi.org/10.1002/cphc.202300749

Chemistry Europe
European Chemical Societies Publishing

www.chemphyschem.org

^{13}C CSA Tensors and Orientational Order of Model and Dimer Mesogens Comprising of Phenyl Benzoate

Gallelli Pratap,[a, d] Yanati Santhosh K. Reddy,[a] Nitin P. Lobo,[b, d] Krishna V. Ramanathan,[c] and Tanneru Narasimhaswamy*[a, d]

A Model mesogen and its symmetrical Dimer made up of phenyl benzoate core unit are investigated by ^{13}C NMR spectroscopy. The existence of layer order in smectic A and smectic C phases of Dimer mesogen is established by powder X-ray diffraction. The chemical shift anisotropy (CSA) tensors of Model mesogen are determined by 2D separation of undistorted powder patterns by effortless recoupling (SUPER) experiment and are utilized for calculating the order parameters employing the alignment-induced chemical shifts (AIS). Additionally, 2D separated local field (SLF) NMR is availed for extracting ^{13}C-^{1}H dipolar couplings for both mesogens and used for computing the order parameters. A good agreement in the order parameters calculated from ^{13}C-^{1}H dipolar couplings and AIS is observed. Accordingly, the main order parameter (S_{zz}) for the phenyl rings of the Model mesogen is found to be in the range 0.54–0.82, and for the Dimer mesogen, the values span 0.64–0.82 across mesophases. Since the phenyl benzoate core unit is frequently employed structural moiety for constructing the main chain as well as side chain liquid crystalline polymers and liquid crystalline elastomers, the CSA tensors reported here will be of immense utility for the structural characterization of these materials.

Introduction

Phenyl benzoate is a widely exploited core moiety for the main chain and side chain liquid crystalline polymers, and similarly in the recently prevalent liquid crystalline elastomers.[1,2] In this context, the study of dimers which are built with two rigid core units linked through flexible spacers is quite fascinating.[3] The research interest in liquid crystal dimers began relatively recently in contrast to polymers. The dimers are considered as true model systems for main chain liquid crystalline polymers which are endowed with a unique balance of orientational, mechanical, magnetic, optical, and electrical properties, high toughness, low die swell, easy flowability, outstanding chemical and thermal resistance, high modulus, and excellent dimensional stability.[4,5] However, the research revealed that the dimers have evolved as a distinct class of mesogens with their unique mesophase properties and molecular organization depending on the odd-even parity of the spacer, the mesogenic properties vary widely.[6] For example, the studies on the transition temperatures of a wide range of dimers disclosed that they directly depend on the odd-even parity.[3,6] This is owing to the fact that the gross molecule shape is rod-like for dimers built with even spacer whereas for odd dimers bent shape is found.[7] As a consequence, profound changes in mesophase properties have been observed.[8,9] Recently found twist-bend nematic (N_{TB}) mesophase in odd dimers has sparked enormous interest in researchers.[10] In the N_{TB} phase, the director exhibits periodic twist and bend deformations forming a conical helix with doubly degenerate domains having opposite handedness.[11,12]

The orientational order is the defining property of liquid crystalline molecules and it measures the tendency of the molecules to be correlated even when separated by large distances.[13] Nuclear Magnetic Resonance (NMR) spectroscopy has been extensively used not only for structural characterization but also for probing molecular dynamics.[14] Particularly, ^{1}H, ^{2}H, ^{13}C, and ^{19}F nuclei have been widely employed for the study of mesogens in the liquid crystalline phase.[15] In recent years the orientational order parameters measured by NMR spectroscopy are employed for finding the molecular topology of the mesogens.[16] For instance, the rod-like and bent-core topology of mesogens can be easily established by considering the ratios of main order parameters (S_{zz}) of constituent rings.[17,18] The ^{13}C NMR in particular found utility for examining the topology of a wide range of molecular mesogens using the order parameters.[19–21] The measurement of order parameters requires information about the chemical shift values of the carbons of the core unit in mesophase as well as the chemical shift anisotropy (CSA) tensors or the ^{13}C-^{1}H dipolar couplings.[22] When CSA tensor information is accessible for the core unit carbons of the mesogens, it becomes possible to determine the orientational order parameters directly from the alignment-induced chemical shifts (AIS).[23] While the ^{13}C-^{1}H dipolar couplings measured from the 2D separated local field (SLF) of mesogens in the liquid crystalline phase can also be employed for finding the order parameters, these experiments are time-

[a] G. Pratap, Y. S. K. Reddy, T. Narasimhaswamy
Polymer Science and Technology, CSIR-Central Leather Research Institute, Adyar, Chennai-600020, India
E-mail: tnswamy99@hotmail.com

[b] N. P. Lobo
Centre for Analysis, Testing, Evaluation & Reporting Services (CATERS), CSIR-Central Leather Research Institute, Adyar, Chennai-600020, India

[c] K. V. Ramanathan
NMR Research Centre, Indian Institute of Science, Bangalore 560012, India

[d] G. Pratap, N. P. Lobo, T. Narasimhaswamy
Academy of Scientific and Innovative Research (AcSIR), Ghaziabad-201002, India

consuming.[24] In this work, a detailed ^{13}C NMR investigation of Dimer and its Model mesogen made up of phenyl benzoate is undertaken to report the order parameters of core units. For this purpose, the CSA tensors determined by 2D separation of undistorted powder patterns by effortless recoupling (SUPER) experiments of Model mesogen are utilized.[19,25] Also, the ^{13}C chemical shifts of Model mesogen are used for assigning the chemical shifts of the Dimer which eliminates the uncertainty in the chemical shift assignment. Finally, the order parameters of the core units determined from ^{13}C chemical shifts are compared with those obtained from ^{13}C-^{1}H dipolar couplings at two representative temperatures across the mesophase and a reasonable agreement is inferred.

Results and Discussion

The molecular structures of the Model mesogen as well as the Dimer mesogen are shown in Figure 1. The synthetic outline employed for realizing both mesogens and details related to analytical data is furnished in the Supporting Information. The mesophase properties of Model mesogen are reported in the literature and accordingly, it exhibits nematic, smectic A (SmA), and smectic C (SmC) mesophases.[26,27] The mesophase transition temperatures for the Model mesogen are crystal-SmC (72.8 °C), SmC-SmA (81.0 °C), SmA-nematic (82.0 °C), and nematic-isotropic (89.1 °C) and are in consistence with the literature data.[26,27] A considerable quantum of data is accessible from the literature on the synthesis and mesophase properties of homologs of Dimer mesogen.[28,29] However, for the Dimer examined in the present work, the mesophase characteristics are not reported in the literature and hence are evaluated by hot-stage optical polarising microscope (HOPM), differential scanning calorimetry (DSC), and X-ray diffraction (XRD) techniques. Griffin and Britt christened the homologs of the Dimer mesogen (Figure 1) as Siamese-twin diesters earlier.[28] These Siamese-twin diesters drew attention due to their molecular structure is intermediate between low molar mass liquid crystals and polymeric analogs. Griffin and Britt further examined the mesophase characteristics of 4-alkoxyphenyl −4′-alkoxy benzoates which in turn serve as model molecule to Siamese-twin diesters.[29] Later, Jin et al. extended the work on Siamese-twin diesters and employed them as structural models for main liquid crystalline polyesters which is their foremost interest.[30,31] They found smectic mesophases besides the nematic phase depending on the length of the spacer and terminal chain.[30] The Dimer mesogen examined in the present work is realised by linking C8 spacer to two ring-based phenyl benzoate core units belonging to Siamese-twin esters family (Figure 1).[28–30] Further, the Model mesogen examined is a low molar mass liquid crystal namely 4-(dodecyloxy)phenyl 4-(octyloxy)benzoate[26,27] which aids as archetypal for the Dimer mesogen (Figure 1).

The motivation for undertaking the current investigation on a Model as well as Dimer mesogens is that the phenyl benzoate core unit is an important moiety extensively employed for synthesizing liquid crystalline polymers.[31–34] Further, the recent thrust on liquid crystalline elastomers which are stimuli-responsive materials known for their ability to generate large, complex deformations in response to impetus are usually constructed with mesogens made up of phenyl benzoate-based core units.[2,35,36] Therefore, detailed ^{13}C NMR studies of the model as well as dimer mesogens provide CSA tensors and the ordering trend of the core unit which in turn would be useful for probing the main chain liquid crystalline polymers and liquid crystalline elastomers based on phenyl benzoate.

The work is described in two parts: (i) determination of the orientational order parameter using ^{13}C chemical shifts with the help of CSA tensors calculated from the 2D SUPER method and (ii) finding the order parameter from ^{13}C-^{1}H dipolar couplings extracted from 2D SLF NMR for the Model as well as Dimer mesogens and compare the values. Since the Model mesogen, as well as the Dimer mesogen, own structurally similar core units, the CSA values of the Model mesogen are utilized to determine the order parameters of the Dimer mesogen. The rationale for employing both 1D and 2D ^{13}C NMR experiments is based on the fact that the 2D experiments typically demand an extended period of NMR spectrometer time in contrast to the 1D experiments.

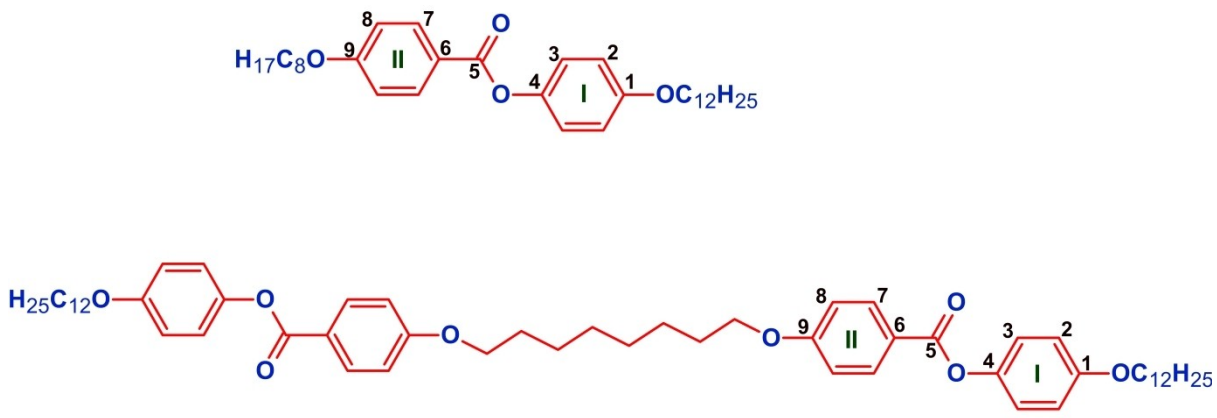

Figure 1. Molecular structures of (A) Model and (B) Dimer mesogens with carbon numbering of core unit

HOPM, DSC and XRD Studies of Dimer Mesogen

The mesophase properties of Dimer mesogen are examined by HOPM. On cooling the isotropic phase of the Dimer sample, in HOPM, somewhat unusual textural features are noticed. Quite interestingly the simultaneous formation of different types of birefringent shapes is observed. Accordingly, the formation of birefringent spherical droplets along with curved stripes is observed at 155.0 °C (Figure 2A). On slow cooling (1 °C/min), the growth of the spherical droplets is noticed (154.5 °C). Further, the curved stripes experienced an evolution and suddenly curled up. The droplets on the other hand elongated to cylindrical structures. On further cooling, the cylindrical structures suddenly collapsed leading to the formation of focal conic defects characteristic of SmA phase at 153.5 °C (Figure 2B).[37] These kinds of rare textures for the SmA phase are reported in the literature for different types of mesogens including Dimers.[38–41] For instance, Prathibha and Madhusudana noticed uncommon texture for SmA mesophase in some binary mixtures and proposed that the curvature of smectic layers is responsible for the unusual texture.[38] The Dimer mesogen on continued cooling, at 129.6 °C textural change is noticed indicating phase change (Figure 2C). The focal conic fans of the SmA phase transformed into the sanded fan texture of SmC mesophase.[42] Another change is noticed at 108.8 °C where striations across the texture are observed (Figure 2D). These mesophase transitions are further confirmed by DSC measurements. The DSC scan confirms the enantiotropic nature of the mesophases as the transitions are observed both on heating and cooling cycles (Figure 3). The enthalpy value for the isotropic to SmA phase transition (155.0 °C) is 3.90 kcal/mol while for the SmA to SmC (129.6 °C) phase change, a very low value typical of second-order transition is found. For the transition observed at 108.8 °C, the enthalpy is found to be 1.41 kcal/mol while the one observed at 93.7 °C showed an enthalpy of 9.00 kcal/mol.

The existence of layer order archetype of smectic mesophases is further established by the XRD method.[43–46] The powder XRD profile of the Dimer mesogen measured at 150.0 °C in the SmA phase (Figure 4A) exhibits a sharp and intense peak in the small angle region at $2\theta = 1.62°$ corresponding to layer spacing (d) of 54.53 Å. A low intense sharp peak is observed at $2\theta = 3.25°$ in the small angle region is the harmonic of the intense sharp peak noted at 1.62°. In the wide-angle region, however, a broad hump centered at 19.64° (2θ) is noticed. The appearance of a broad hump at a wide angle region indicates the liquid-like nature of the molecules within the layer and the absence of in-plane order. The XRD profile

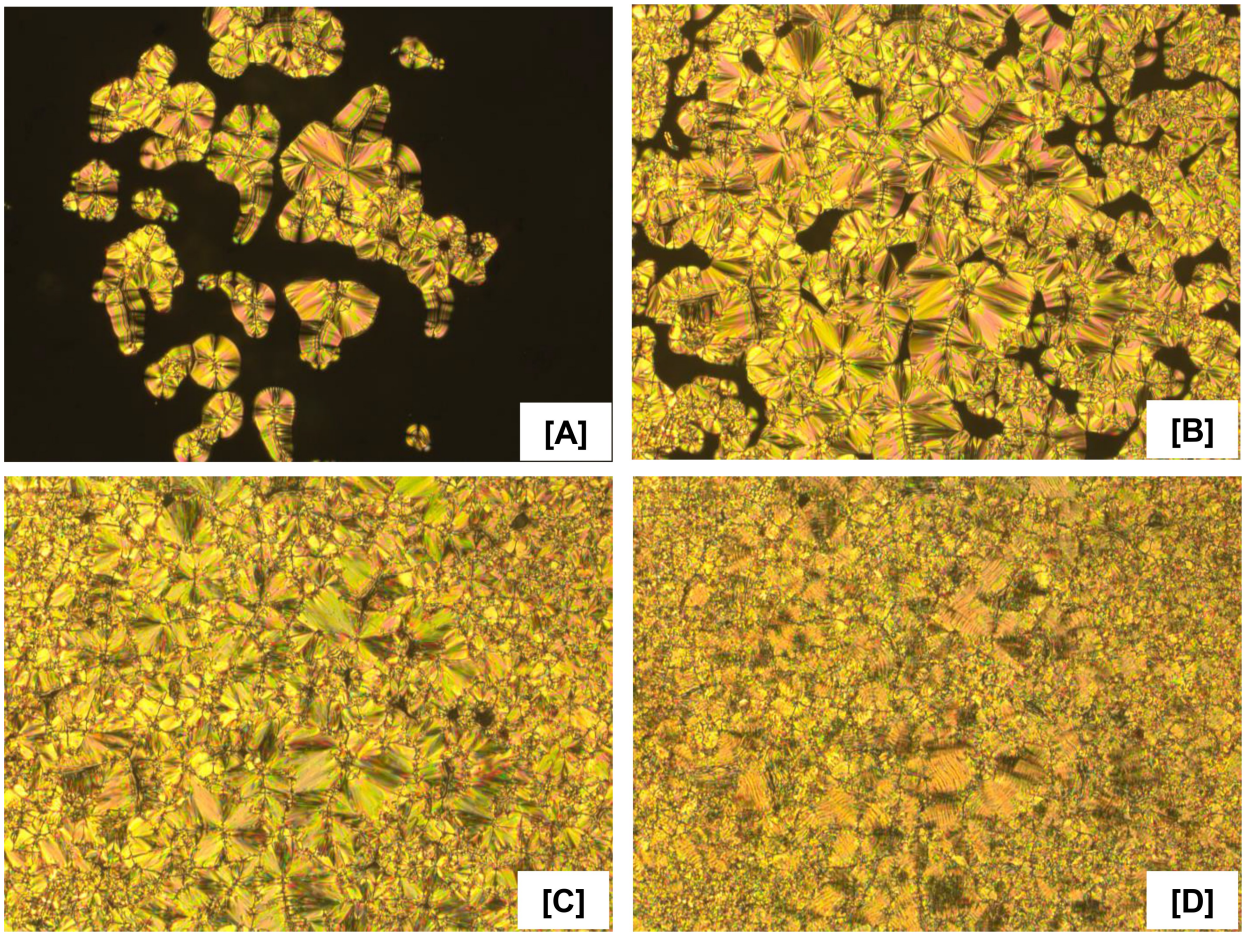

Figure 2. HOPM images of Dimer in SmA Phase (A) 155.0 °C, (B) 153.5 °C; SmC phase (C) 129.6 °C; Crystal phase (D) 107.0 °C

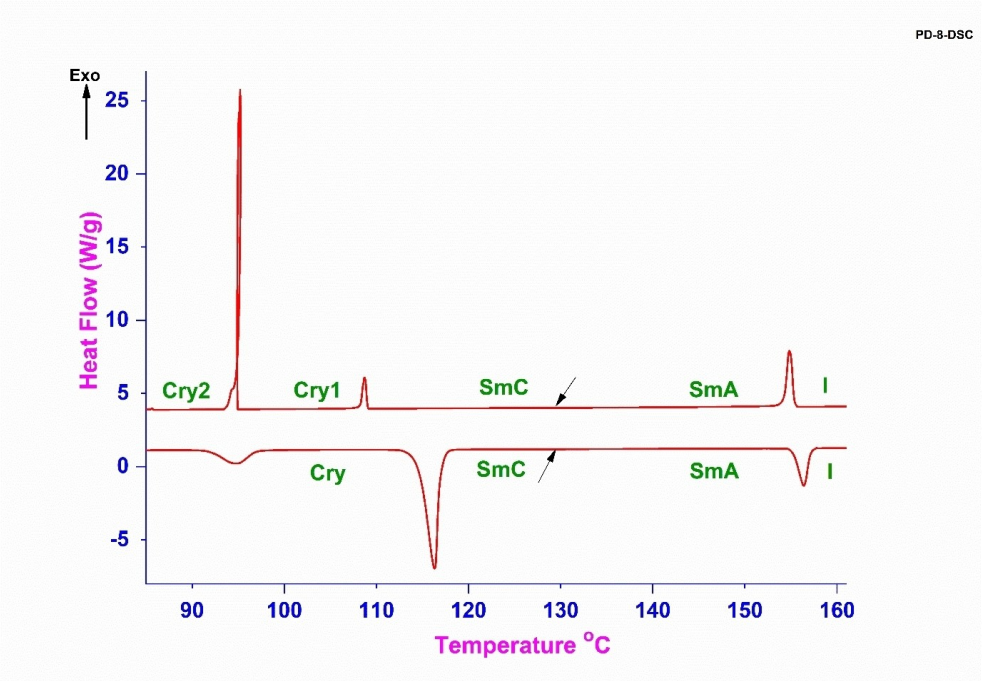

Figure 3. DSC trace of Dimer mesogen; second heating/cooling curve with a heating rate of 10 °C/min

measured at 125.0 °C in the SmC phase shows a shift in the small angle reflections (Figure 4B). Accordingly, in the small angle region sharp and intense peak is noted at 1.67° (2θ) and its second harmonic at 3.35° (2θ). In the wide-angle region similar to the SmA phase, a broad hump is noted (2θ = 19.82°). Thus both SmA and SmC XRD scans are very much consistent with the features associated with fluid smectic phases.[47,48] The change in the location of the small angle peak for SmC mesophase supports the tilted nature of the molecules in the layer. The appearance of second-order reflection in the small angle region for both SmA and SmC mesophases supports the better layer interface. To understand the nature of the transition observed at 108.8 °C in DSC, the XRD study is carried out for the sample at 105.0 °C (Figure 4C) where many changes are noticed. In the small angle region, numerous peaks are observed with varying intensity. Further, the broad hump witnessed at the wide angle region for both SmA and SmC phases is replaced by several peaks with dissimilar intensities. The highly intense peaks noted in the small angle region at 2θ = 1.62° and 3.23° indicate the persistence of layer order while the large number of peaks observed at the wide-angle region denotes the crystalline nature of the phase. The molecular length (L) of the Dimer calculated from the density functional theory method of quantum chemical calculations is 64.88 Å. Significantly, in the SmA phase for the Dimer mesogen, the layer spacing and molecular length (d/L) ratio is found to be 0.84 ($0.5 < d/L < 1$). Usually, the layer spacing (d) in the SmA phase is comparable to molecular length (L) for a monolayer orthogonal smectic phase, and a slight deviation from d/L = 1 is attributed to the orientational disorder of the terminal chains.[49,50] In the present study, for the Dimer in the SmA phase, the difference between d and L is fairly high (d-L is 10.35 Å). A large difference between d and L is also observed for dimers/oligomers in the SmA phase in a few cases as evidenced by the literature. For instance, Chan et al. in the study of the SmA phase of symmetrical trimers observed a d/L ratio of 0.75–0.80 for short homologues.[51] They accounted the unusual d/L ratio owing to the intercalation of parts of the terminal chains up to a few carbons. In addition, they argued that the intercalation of terminal chains is a known factor favoring the SmC phase in liquid crystal dimers. Further, Grunwald et al. while examining the cyanobiphenyl dimers with a central malonate unit noticed variation between d and L to the tune of 10.7 Å in the SmA phase.[52] To explain the large difference in experimentally determined layer spacing (d) and molecular length (L), they proposed two different molecular organizations in which one model describes the antiparallel interdigitation of cyanobiphenyl moieties and another one invokes the hairpin conformation. Yelmaggad and Shanker,[53] Liao et al.[54] also observed similar instances of low d/L ratio for the SmA phase and proposed intercalated structure for the symmetrical dimers. In view of literature studies on dimers and the occurrence of similar d/L ratio noted for the Dimer under study, we propose a model for SmA mesophase in which the few carbons of the terminal dodecyloxy chains intercalate into neighboring layers. As a consequence, the experimentally determined layer spacing (54.53 Å) measured in the SmA phase (150 °C) of the Dimer is taken to match to the intercalated structure. Accordingly, the tilt angle in the SmC phase for the Dimer is found to be 13.7°. The tilt angle is calculated by using the expression $d_C/d_A = \cos\theta^{-1}$ where d_C is the layer spacing in the SmC phase (52.98 Å) and d_A is the layer spacing in the SmA phase (54.53 Å) of the Dimer.

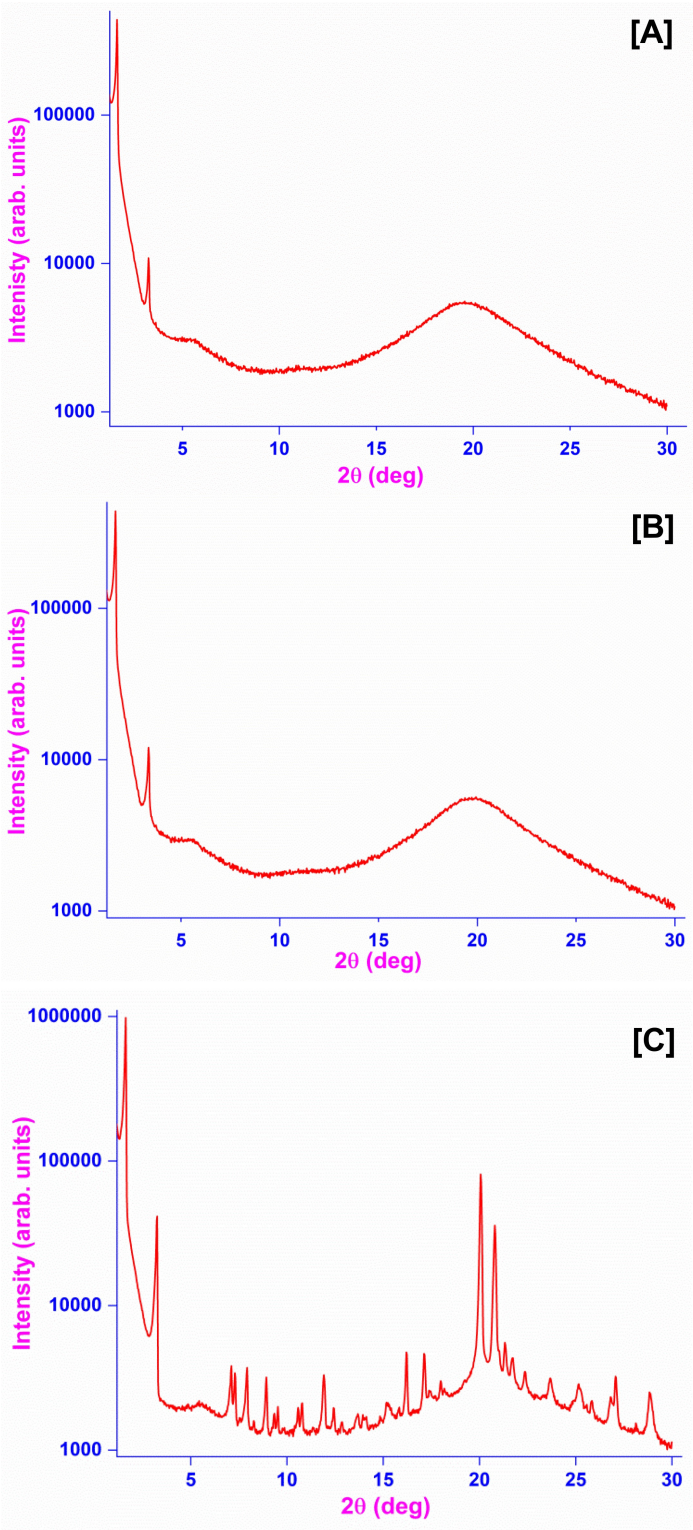

Figure 4. XRD profiles of Dimer mesogen in (A) SmA phase (150.0 °C), (B) SmC phase (125.0 °C) and (C) Crystal phase (105.0 °C)

^{13}C NMR Investigations of Mesogens

The determination of CSA values for Model mesogen and order parameters for the core unit of the Dimer would be of immense utility for the ^{13}C NMR studies of the main chain liquid crystalline polymers as well as the liquid crystalline elastomers as indicated earlier. Therefore the present study involves the use of 2D SUPER and 2D SAMPI-4[55] NMR experiments for finding the CSA and ^{13}C-^{1}H dipolar couplings, respectively for the core unit of the Model mesogen. The ^{13}C CSA values

calculated for the Model mesogen are then exploited for the structural assignment of the Dimer mesogen as well as for calculating the order parameters. Further, the ^{13}C-^{1}H dipolar couplings extracted from 2D SAMPI-4 for both mesogens are also utilized to find the order parameters. Since performing the 2D SAMPI-4 experiments typically requires an extended period of NMR spectrometer time, the 1D experiments are carried out across the mesophase range while the 2D experiments are restricted to few temperatures.

^{13}C NMR of Mesogens in Solution

The proton decoupled solution ^{13}C NMR spectrum of Model mesogen is shown in Figure 5A. The spectrum in the region 114.0–163.5 ppm exhibits sharp and well-resolved lines for the two phenyl rings of the core unit. The protonated carbons of the phenyl rings showed sharp and intense lines in the region 114.0–133.0 ppm. The non-protonated carbons, on the other hand, exhibited low intense lines (144.4 to 165.3 ppm) except

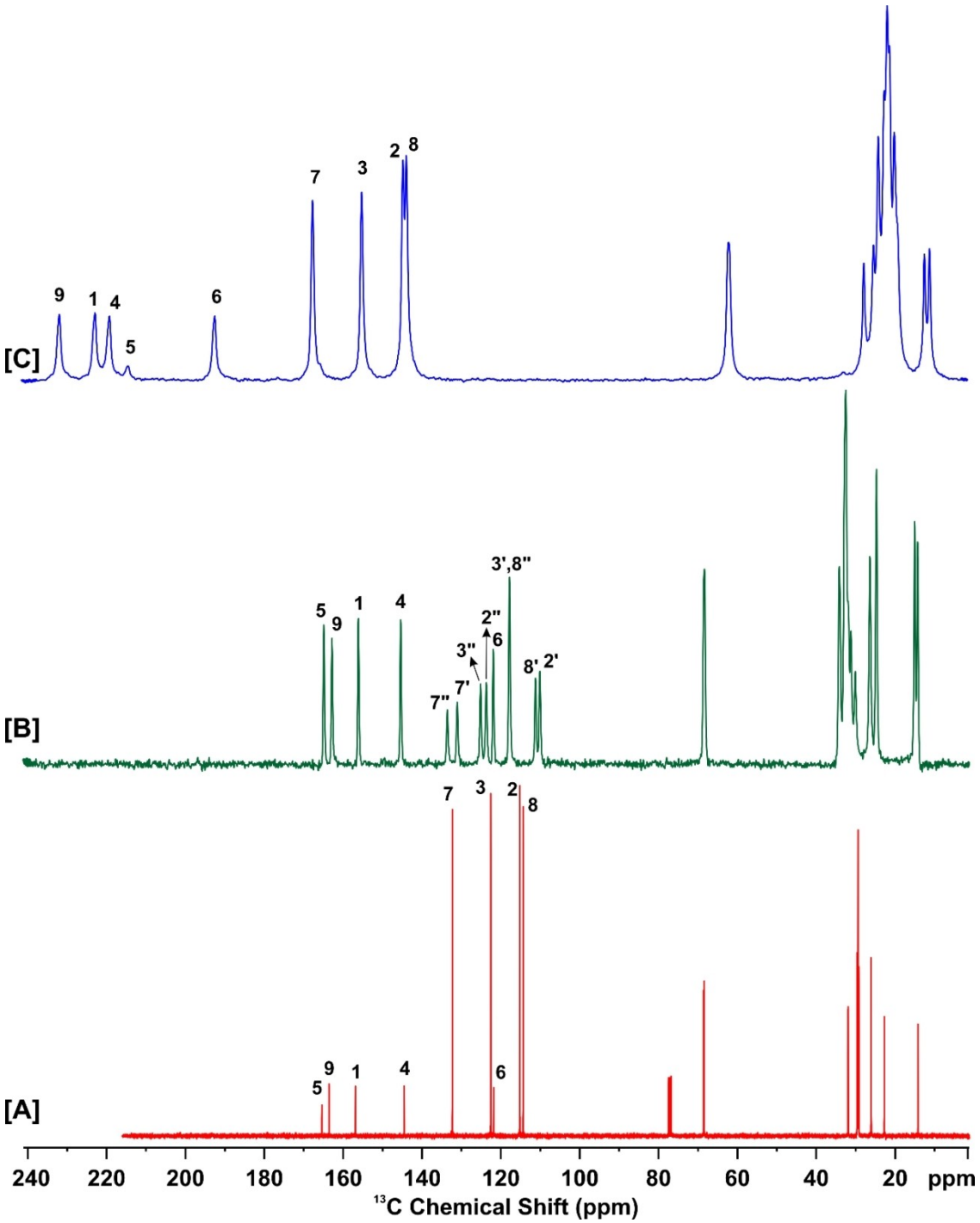

Figure 5. (A) Proton-decoupled ^{13}C NMR spectrum of Model mesogen in solution (B) ^{13}C CPTOSS spectrum in solid phase (5 kHz spinning speed) and (C) ^{13}C CP spectrum in SmC phase under static condition (74 °C).

for the C6 carbon which is noted at 121.7 ppm. The lines pertaining to both terminal alkoxy chains are noted from 14.0 to 68.5 ppm. Thus two lines that appeared at 68.3 and 68.4 ppm are attributed to OCH_2 carbons and the other two lines seen at 14.0 and 14.1 ppm are assigned to methyl carbons of both terminal chains. The rest of the methylene carbons of the terminal chains are observed from 22.5 to 32.0 ppm in which the line appeared at 29.2 ppm is the most intense. The assignment of the carbons is accomplished by comparing the data of structurally similar molecules available from the literature.[56] Table 1 lists the chemical shift values of the core unit carbons of the Model mesogen.

Figure 6A shows the proton decoupled ^{13}C NMR spectrum of Dimer mesogen in solution. Similar to Model mesogen, the spectrum in the range 114.0–165.5 ppm shows sharp and intense lines for the phenyl ring carbons of the core unit. Among them the protonated carbons appeared from 114.0 to 133.0 ppm are more intense than other lines. The non-protonated carbons are seen from 144.4 to 165.3 ppm with low intensity. The C6 carbon, however, showed a line at 121.9 ppm. For the spacer and terminal chain carbons, the lines are noted from 14.0 to 68.4 ppm in which the OCH_2 carbons are observed at 68.0 and 68.4 ppm while the terminal methyl is seen at 14.0 ppm. The assignment of the spectral lines is accomplished by comparing the ^{13}C NMR data of the Model mesogen. Table 1 lists the chemical shift values of core unit carbons of the Dimer mesogen. It is very clear from Table 1 that the structural similarity between the Model mesogen and the Dimer mesogen is very much reflected in the chemical shift values

^{13}C NMR Study of Model Mesogen in Solid Phase

As stated earlier, the 2D SUPER experiments are performed for the Model mesogen in the solid phase to find the CSA tensor components of core unit carbons which in turn are used for calculating the order parameters in the liquid crystalline phase. In order to get the CSA values from the SUPER experiment, initially the ^{13}C NMR spectrum in the solid state for Model mesogen is realized by spinning the sample at 5 kHz at room temperature using a ^{13}C CPTOSS sequence.[57] The spectrum in Figure 5B displayed 12 sharp peaks with varying intensity in the chemical shift range 110.0–165.0 ppm for the core unit carbons in contrast to 9 lines in the solution spectrum (Figure 5A). Further slight variation in chemical shifts is observed in the spectrum due to solid-state packing effects.[58,59] To assign the peaks, the CPPI spectral editing experiment[60] (Figure S1 in Supporting Information) is carried out to differentiate between protonated and non-protonated carbons. Consequently, the non-protonated carbons exhibited signals with a positive phase, while methylene carbon peaks exhibited a negative phase, and protonated carbons were effectively eliminated.

As mentioned before, there are more peaks in the solid state in comparison to the spectrum in solution and the mesophase. A reason for the appearance of multiple peaks in the solid state could be the presence of more than one molecule in the asymmetric unit cell. However, the non-protonated carbons which are more susceptible due to their relatively large chemical shift anisotropy, do not show evidence of this. Hence it is concluded that the freezing of 180° flips about the para axis and consequent non-equivivalence of carbons at ortho and meta positions are responsible for the doubling of the corresponding spectral lines. The assignment of these split resonances in the solid state has been done by considering the mean of the peak positions and matching it with the nearest peak in the solution. Table 1 lists the chemical shifts of the core unit carbons along with values arising from splitting. Importantly, the splitting of carbon signals vanishes when the sample is heated to a liquid crystalline phase as discussed in the following section.

Table 1. ^{13}C NMR data for Model and Dimer mesogens in different phases.[a]

	Model								Dimer						
C. No.	Soln. (ppm)	CP/TOSS (ppm)	Smectic C (74 °C)			Nematic (83 °C)			Soln. (ppm)	Smectic C (110 °C)			Smectic A (135 °C)		
			CS (ppm)	AIS (ppm)	DOF (kHz)	CS (ppm)	AIS (ppm)	DOF (kHz)		CS (ppm)	AIS (ppm)	DOF (kHz)	CS (ppm)	AIS (ppm)	DOF (kHz)
1	156.8	156.1	221.5	64.7	1.90	213.6	56.8	1.73	156.8	222.9	66.1	1.81	218.2	61.4	1.62
2	115.1	110.1 123.7	144.0	28.9	2.97	140.5	25.4	2.58	115.1	144.0	28.9	2.85	142.1	27.0	2.75
3	122.4	117.7 125.1	154.3	31.9	2.78	150.3	27.9	2.44	122.4	153.6	31.2	2.67	151.1	28.7	2.53
4	144.4	145.3	217.8	73.4	1.86	208.6	64.2	1.65	144.4	219.0	74.6	1.84	213.8	69.4	1.69
5	165.3	164.8	213.3	48.0	1.37	–	–	–	165.3	213.8	48.5	0.36	210.0	44.7	0.26
6	121.7	121.8	191.3	69.6	1.82	182.9	61.2	1.57	121.9	193.9	72.0	1.93	189.1	67.2	1.79
7	132.2	130.9 133.6	166.8	34.6	2.69	162.5	30.3	2.38	132.2	166.1	33.9	2.74	163.6	31.4	2.62
8	114.2	111.1 117.7	143.2	29.0	2.80	139.7	25.5	2.42	114.3	143.0	28.7	2.81	141.1	26.8	2.70
9	163.4	162.8	230.5	67.1	1.85	222.2	58.8	1.69	163.4	232.8	69.4	1.90	228.2	64.8	1.76

[a] Soln.: solution chemical shift, CS: mesophase chemical shift; AIS: alignment-induced chemical shift; DOF: ^{13}C-^{1}H dipolar oscillation frequencies

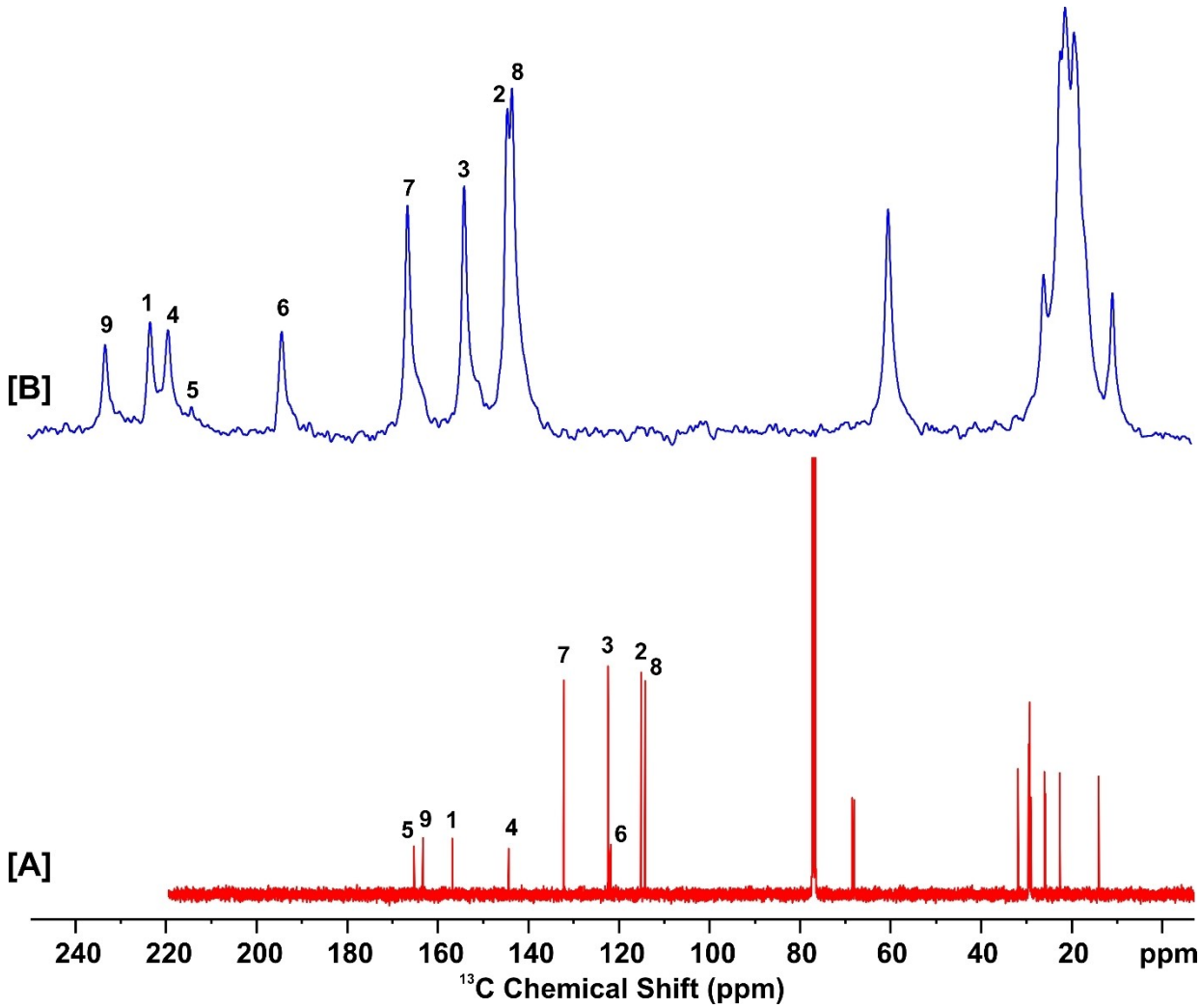

Figure 6. (A) Proton-decoupled ^{13}C NMR spectrum of Dimer mesogen in solution and (b) ^{13}C CP spectrum in SmC phase (110 °C).

2D SUPER Experiment for Model Mesogen

The 2D ^{13}C chemical shift anisotropic-isotropic correlation SUPER spectrum of Model mesogen in the solid phase is shown in Figure 7. The CSA of core unit carbons is only considered since the main attention is to estimate the orientational order parameter of the molecule in the liquid crystalline phase. Figure 8 depicts the CSA powder pattern (blue dotted lines) of different aromatic carbons extracted from F1 cross sections from Figure 7. To estimate the principal values of CSA tensors, the experimental powder line shapes are simulated using the WSOLIDS package[61] and the simulated spectra are shown as red color solid lines for direct comparison (Figure 8). The principal components of the CSA tensor (δ_{11}, δ_{22} and δ_{33}) are labelled by the IUPAC rules and follow $\delta_{11} \geq \delta_{22} \geq \delta_{33}$ sequence (Mehring convention) where $\delta_{iso} = (\delta_{11} + \delta_{22} + \delta_{33})/3$.[62] The obtained CSA values for aromatic carbons are listed in Table 2. As noted earlier, all four protonated carbons namely C2, C3, C7, and C8, show splitting of the peaks, and accordingly, the corresponding CSA values are listed in Table 2. It is important to note that, because of motional averaging, both peaks observed for each carbon in the solid phase combine into a single peak in solution as well as in liquid crystalline phases. Consequently, in the isotropic (solution) phase, the chemical shift value of the peak corresponds to the average of the two peaks observed in the solid phase. In contrast, in the liquid crystalline phase, the peak manifests at a higher chemical shift value. Table 2 also lists the average values of CSA of core unit carbons of Model mesogen.

^{13}C NMR Studies of Mesogens in the Liquid Crystalline Phase

As stated previously, the Model mesogen exhibits nematic, SmA (short interval), and SmC mesophases. The static ^{13}C NMR measurements are performed both in nematic and SmC mesophases and for the discussion, the spectrum measured in SmC phase is considered. The static ^{13}C NMR spectrum (Figure 5C) shows 9 peaks with varying intensities in the range of 143.0–230.5 ppm. The protonated carbons of the phenyl ring of the core unit are seen in the span 143.0–167.0 ppm. The non-protonated carbons of the phenyl ring as well as the ester

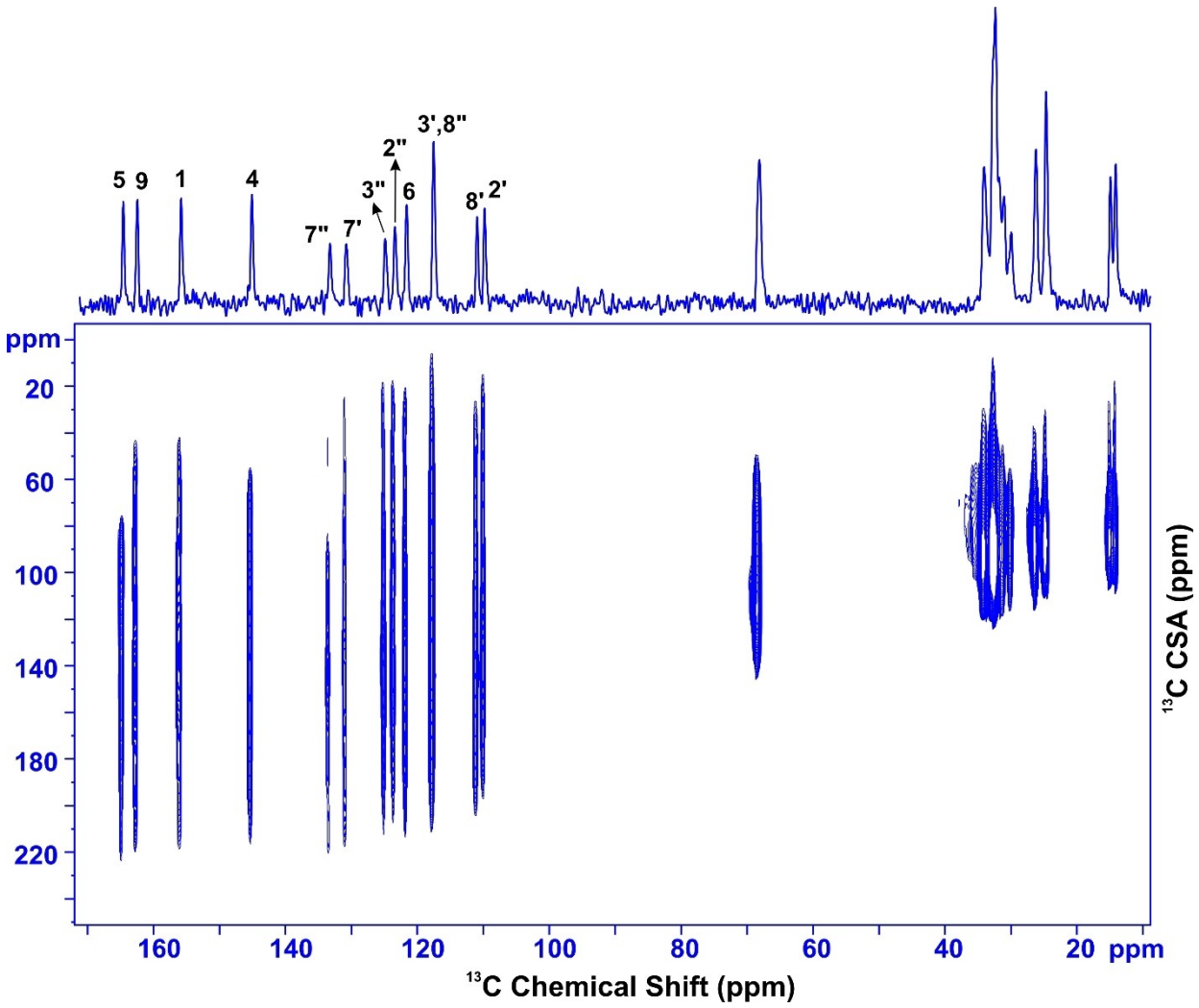

Figure 7. 2D SUPER spectrum (sheared) in the solid phase of Model mesogen

carbonyl carbons are observed from 191.0 to 230.5 ppm. For the terminal chains, the peaks are seen in the range of 10.5–62.0 ppm. Among them, the peak that appeared at 61.7 ppm is attributed to oxymethylene carbons while the methylene carbons are seen in the range 19.0–27.5 ppm. The terminal methyl carbons, on the other hand, are noted at 12.0 and 10.8 ppm. The 1D static ^{13}C NMR experiments are carried out at various temperatures covering both nematic and SmC mesophases. This allowed us to determine the order parameters as a function of temperature by making use of CSA values collected from the 2D SUPER experiment as discussed later. From the measurements, the AIS values are calculated at different temperatures by using the expression $\delta_{lc}-\delta_{soln}$ where δ_{lc} and δ_{soln} are the chemical shifts in the liquid crystalline phase and solution, respectively.[23] Table 1 lists the data pertaining to chemical shifts and AIS values for the core carbons of the Model mesogen. It is clear from the ^{13}C NMR chemical shifts as well as the order parameter data discussed later that the molecules are aligned along the magnetic field in both phases.[22,63] Accordingly the chemical shift values of core unit carbons showed an increase in chemical shifts in the liquid crystalline phase while for the terminal chain carbons, a marginal decrease in contrast to solution ^{13}C NMR chemical shifts is observed.

The 2D SAMPI-4 spectrum of Model mesogen measured in SmC mesophase is shown in Figure 9A. The spectrum shows 9 contours for the core unit carbons in the range 143.0–230.5 ppm. The protonated carbons of the phenyl rings of the core unit showed four contours in the range 143.0–167.0 ppm with ^{13}C-^{1}H dipolar couplings of 2.69–2.97 kHz. In these contours, two are very closely spaced (143.2 and 144.0 ppm) with comparable intensity. For the ester carbonyl carbon, a low intense contour is observed at 213.3 ppm while for the non-protonated carbons of both the rings, the contours are equal in intensity and ^{13}C-^{1}H dipolar couplings ranged from 1.82 to 1.90 kHz. Table 1 lists the ^{13}C chemical shifts along with ^{13}C-^{1}H dipolar couplings of the core unit of mode mesogen.

As stated earlier, the Dimer mesogen exhibits SmA and SmC mesophases. The static ^{13}C NMR of Dimer mesogen measured in the SmC phase at 110.0 °C is shown in Figure 6B. The spectrum in the range of 143.0–233.0 ppm shows well-resolved peaks for the core unit carbons. Of them, four peaks noted in the range 143.0–166.5 ppm are highly intense which are due to proto-

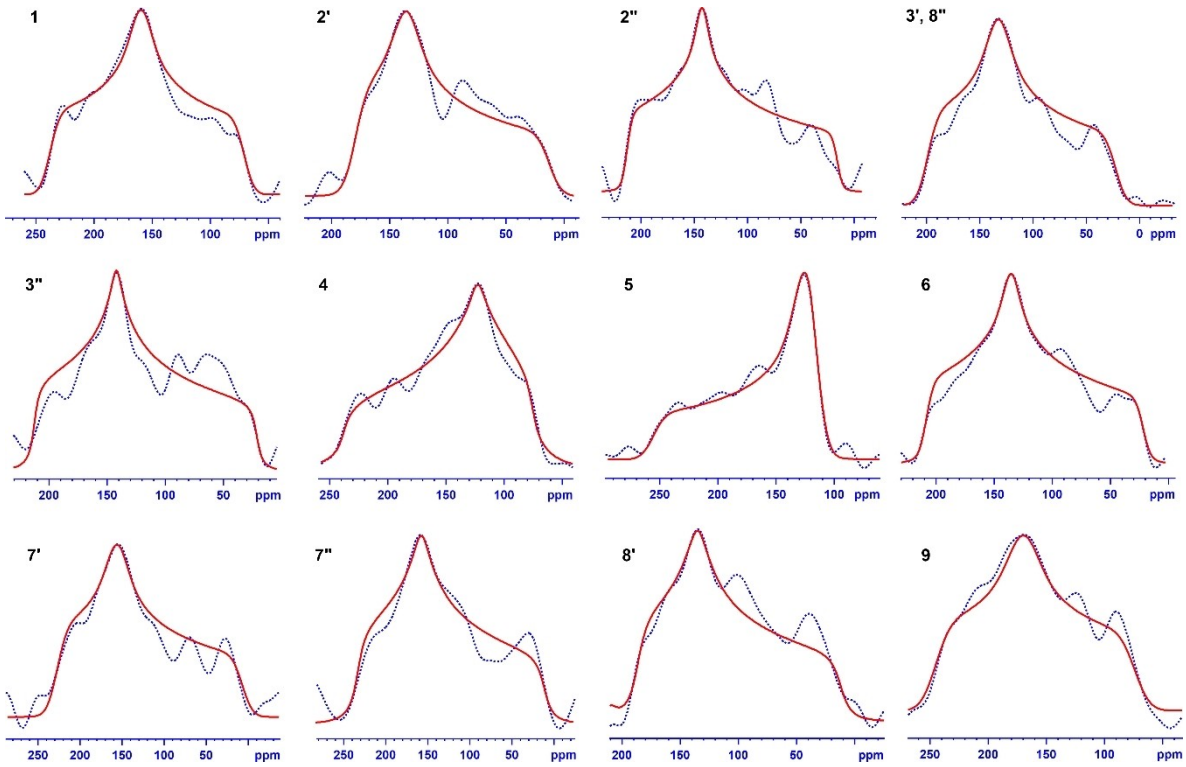

Figure 8. ^{13}C CSA cross-sections for individual phenyl ring carbon sites are extracted from the SUPER experiment. Dotted lines (blue) are experimental values while the solid lines (red) are simulated CSA powder patterns.

Table 2. CSA tensor values for aromatic carbons of Model mesogen in solid phase.[a]

C. N.	CSA (ppm)			
	δ_{11}	δ_{22}	δ_{33}	δ_{iso}
1	238	160	71	156
2′	181	136	13	110
2″	213	143	15	124
2(average)	197	139	14	117
3′	201	132	20	118
3″	212	142	21	125
3(average)	207	137	21	121
4	238	123	75	145
5	256	120	120	165
6	208	135	22	122
7′	230	157	6	131
7″	233	157	10	134
7(average)	232	157	8	132
8′	187	135	12	111
8″	201	132	20	118
8(average)	194	134	16	114
9	245	170	73	163

[a] Uncertainty in the experimental values are ±5 ppm for protonated carbons and ±3 ppm for non-protonated carbons

nated carbons of the phenyl rings of the core unit. The non-protonated carbons of the core unit exhibited chemical shifts in the range 190.0–233.0 with medium intensity. For the spacer as well as terminal chain carbons, the peaks are noted from 10.0 to 60.0 ppm. The peak observed at 60.0 ppm is assigned to OCH_2 carbons and the methyl carbon of the terminal chain is seen at 10.5 ppm. Importantly, in solution ^{13}C NMR spectrum, two lines are seen for OCH_2 carbons whereas in the static spectrum, only one peak is noted. For methylene carbons of the spacer as well as terminal chain, the peaks are noticed in the range of 16.0–26.0 ppm. The alignment of molecules in the magnetic field is ascertained from the chemical shift values of the static ^{13}C NMR spectrum. Similar to Model mesogen, the static ^{13}C NMR experiments for Dimer mesogen are also carried out at a wide temperature range covering both mesophases. Table 1 lists the chemical shifts and AIS values of Dimer mesogen both in the SmA and SmC phases.

The 2D SAMPI-4 spectrum of Dimer mesogen measured in the SmC phase (110.0 °C) is shown in Figure 9B. The spectrum shows well-resolved contours for all the carbons of the core unit. The protonated carbons of the phenyl rings appeared as high intense contours while the non-protonated carbons of the core unit showed lower intensity. The ^{13}C-^{1}H dipolar couplings of the protonated carbons are in the range 2.67–2.85 kHz whereas for the non-protonated carbons of the phenyl rings, the values are in the range 1.81–1.93 kHz. For the spacer and terminal chains, the characteristic OCH_2 contours are seen at 60.0 ppm with ^{13}C-^{1}H dipolar couplings of 7.34 and 6.81 kHz. A close look at the 2D SAMPI-4 spectral data of Model as well as

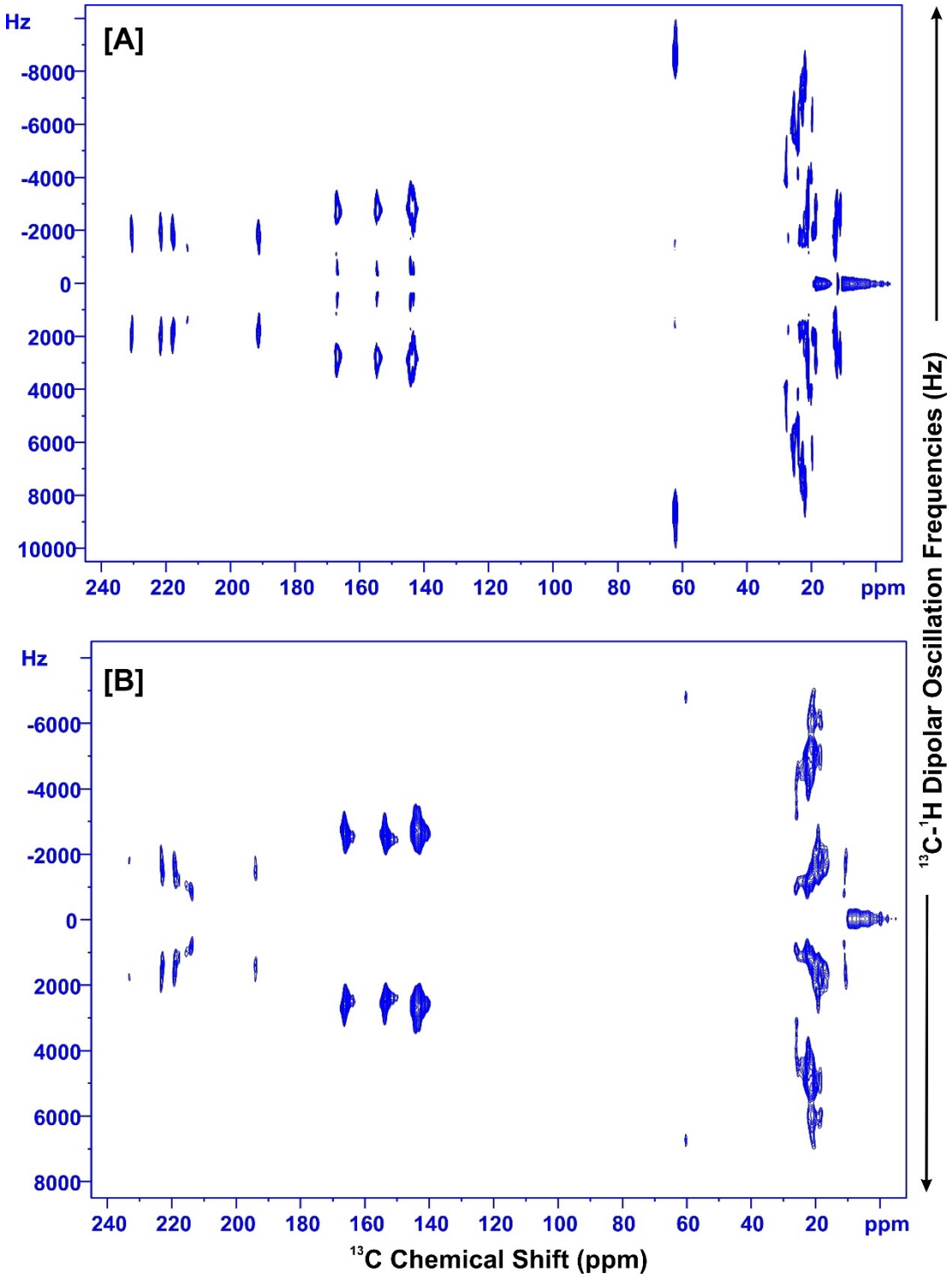

Figure 9. 2D SAMPI-4 spectra of (A) Model mesogen in SmC phase (74 °C) and (B) Dimer mesogen in SmC phase (110 °C)

Dimer mesogens indicate similarity in values not only for chemical shifts but also for the dipolar couplings. Table 1 lists the ^{13}C-^{1}H dipolar couplings of the core unit of the Dimer mesogen in the SmA and SmC phases.

Orientational Order Parameters

In the context of the SAMPI-4 experiment, when dealing with an isolated C–H pair, the measured dipolar oscillation frequency aligns directly with the ^{13}C-^{1}H dipolar coupling. However, when examining carbon atoms linked to multiple protons, the extraction of ^{13}C-^{1}H dipolar coupling information becomes

necessary, requiring consideration of the phenyl ring geometry as previously outlined.[64,65] By adhering to established procedures,[16,17,66] the orientational order parameters for the phenyl rings within the core unit of both mesogens calculated by using the following equation[22,67]

$$D_{C-H} = -h\gamma_C\gamma_H/4\pi^2 r^3_{CH}\ [{}^1/_2\ (3\cos^2\theta_z - 1)\ S_{zz} + {}^1/_2\ (\cos^2\theta_x - \cos^2\theta_y)(S_{xx} - S_{yy})] \quad (1)$$

In the equation, h is Planck's constant, while γ_H and γ_C denote the gyromagnetic ratios of ^{1}H and ^{13}C nuclei, respectively. Additionally, r_{CH} signifies the distance of the C–H bond, and θs are the angles formed between the C–H bond and the coordinate axes defined for the phenyl ring with D_{2h} symmetry. To elaborate, the *z*-axis aligns with the para-axis, while the remaining axes are positioned perpendicular to the *x* and *y* axes, both within and outside the plane of the phenyl ring. For the protonated carbons of the phenyl ring, the experimental dipolar frequency comprises two parts: the coupling with the attached proton at the *ipso* position ($D_{C\text{-}Hi}$) and the coupling with the nearby non-bonded proton at the *ortho* position ($D_{C\text{-}Ho}$). The resulting dipolar frequency was determined as $f = \sqrt{[(D_{C\text{-}Hi})^2 + (D_{C\text{-}Ho})^2]}$. Given that the non-protonated carbons are coupled with two equivalent protons at the *ortho* positions, the dipolar frequency is calculated as $f = \sqrt{2}*(D_{C\text{-}Ho})$. Therefore, the four experimentally measured dipolar oscillation frequencies are employed to fit data and determine the two order parameters, S_{zz} and (S_{xx}-S_{yy}), for the phenyl ring with D_{2h} symmetry. Standard bond distances of $r_{CH} = 1.1$ Å (C–H bond) and $r_{CC} = 1.4$ Å (C–C bond) are utilized during the fitting process. To enhance the accuracy of fit, CCH bond angles slightly varied ~120°.[68] The computed order parameters for the phenyl rings of the core unit of both mesogens are listed in Table 3.

The ^{13}C chemical shifts obtained from several 1D static ^{13}C NMR experiments of Model mesogen in the temperature range 70–91 °C are used for determining the order parameters of the phenyl rings by making use of CSA values extracted from the 2D SUPER experiment. For the Dimer mesogen, since the static ^{13}C NMR data in the temperature range of 105–150 °C is available, the order parameters are calculated utilizing the CSA values of the Model mesogen. The AIS in the liquid crystalline phase is related to the components of the CSA tensor values δ_{ij} and the local order parameters as per the following equation[14]

$$\delta_{lc} - \delta_{soln} = (2/3)\ S_{zz}\ [P_2\ (\cos\beta)\ (\delta_{11} - \delta_{22}) + (1/2)\ (\delta_{22} - \delta_{33})] + (1/3)(S_{xx} - S_{yy})[\delta_{33} - (\cos^2\beta)\ \delta_{22} - (\sin^2\beta)\ \delta_{11}] \quad (2)$$

As stated earlier, the coordinates for the phenyl ring are taken as the z-axis along the para axis of the ring, the x-axis in the plane of the ring, and the y-axis perpendicular to the plane. The angle β is considered 60° for protonated carbons, and 0° for non-protonated carbons of the phenyl ring. Since the phenyl ring possesses D_{2h} symmetry, only two order parameters namely, S_{zz} and (S_{xx}-S_{yy}) are adequate to comprehend the ordering of the ring. Consequently, the four experimentally measured AIS values are used to determine these two order parameters for the phenyl ring.

The order parameters are also calculated for the Model mesogen using ^{13}C-^{1}H dipolar couplings extracted from SAMPI-4 and using Equation (1). The main order parameter (S_{zz}) values for the Model mesogen are 0.80 (ring I) and 0.79 (ring II) in the SmC phase and 0.72 (ring I) and 0.71(ring II) in the nematic phase. Further, the order parameters for Model mesogen are also calculated utilizing Equation (2) since the CSA values and the chemical shifts across the mesophases range are accessible. The plot of S_{zz} versus temperature for Model mesogen is depicted in Figure 10. It is noted from Figure 10 that the order parameter values decrease from 0.82 to 0.54 with an increase in

Table 3. Orientational order parameters for phenyl rings of Model and Dimer mesogens.[a]

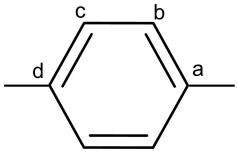

Mesogen	T (°C)	Ring	CCH Bond Angles		S_{zz}	S_{xx}-S_{yy}	Calculated dipolar oscillation frequencies (kHz)				RMSD (kHz)
			θ_b	θ_c			b	c	a	d	
Model	74	I	121.2	121.7	0.80	0.082	2.95	2.78	1.86	1.87	0.02
		II	121.7	121.4	0.79	0.074	2.70	2.80	1.84	1.83	0.01
	80	I	121.4	121.8	0.72	0.071	2.58	2.45	1.67	1.68	0.03
		II	121.7	121.6	0.71	0.062	2.40	2.43	1.64	1.64	0.04
Dimer	110	I	121.3	121.8	0.80	0.073	2.86	2.68	1.84	1.86	0.02
		II	121.9	121.7	0.81	0.082	2.73	2.80	1.90	1.89	0.02
	135	I	120.8	121.5	0.73	0.064	2.76	2.54	1.66	1.68	0.02
		II	121.5	121.2	0.74	0.073	2.62	2.71	1.72	1.71	0.04

[a] In the figure above the table, b and c are protonated carbons and a and d are non-protonated carbons of the phenyl ring.

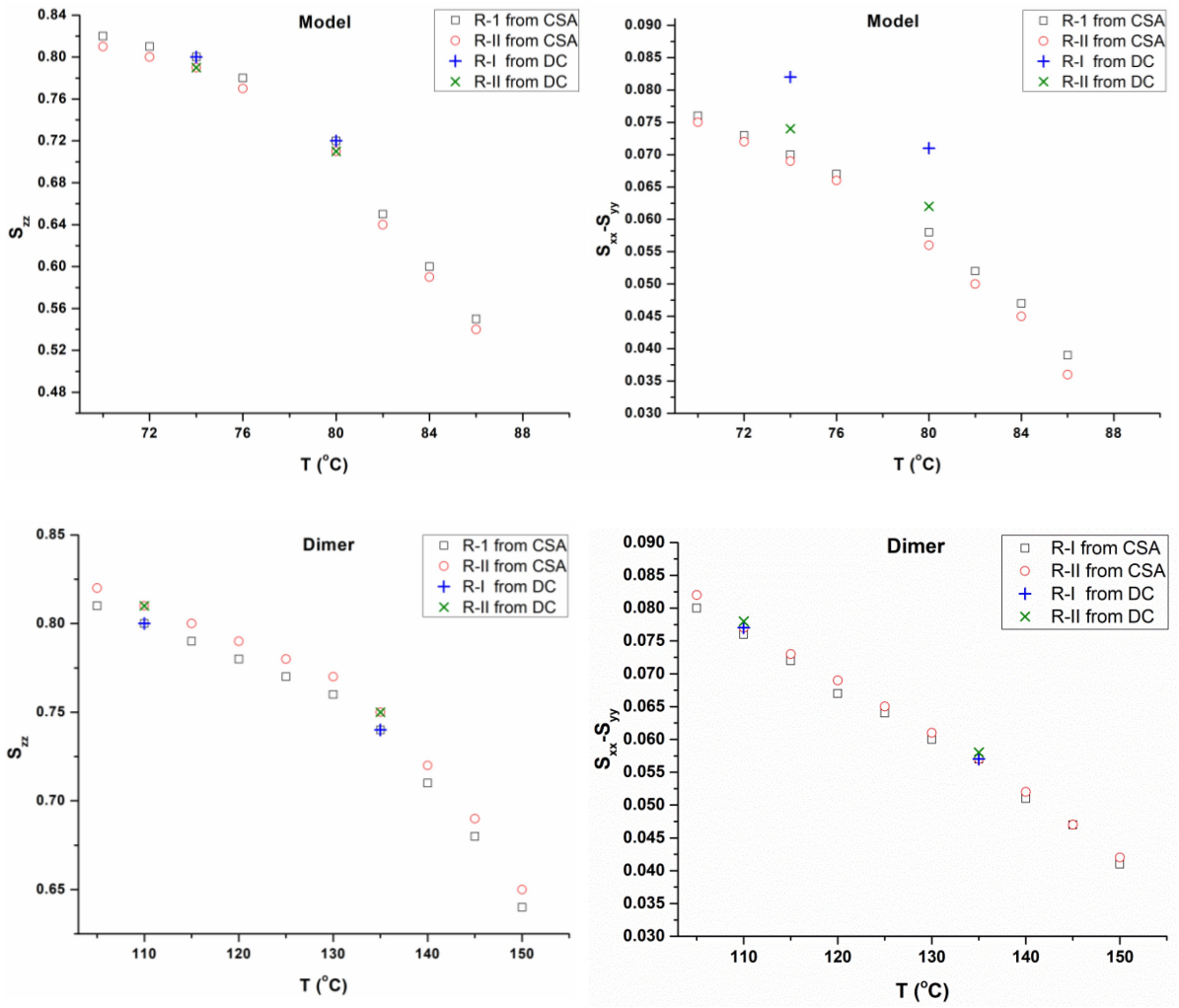

Figure 10. Plots of temperature versus order parameters (S_{zz} and S_{xx}-S_{yy}) for phenyl rings of Model and Dimer Mesogens by using CSA values of Model mesogen. Symbols (+) and (x) represent corresponding order parameters estimated using dipolar couplings for rings I and II, respectively.

temperature from 70 to 86 °C. Similarly, the profile for (S_{xx}-S_{yy}) is also noticed in the measured temperature range. These trends are very much consistent with those observed for rod-like mesogens.[16]

For the Dimer mesogen, the ^{13}C-^{1}H dipolar couplings measured from the 2D experiment are used to estimate the order parameters (Table 3). The main order parameter (S_{zz}) value of ring I in the SmC phase is 0.80 while for ring II the value is 0.81 and in SmA mesophase, the values for both the rings are 0.73 (ring I) and 0.74 (ring II). Additionally, the order parameters for Dimer mesogen are also calculated in the temperature range 105 to 150 °C employing Equation (2) and using the CSA values of Model mesogen (Figure 10). Consequently, the S_{zz} values vary from 0.64 to 0.82 while the (S_{xx}-S_{yy}) values range from 0.041 to 0.082 in SmA and SmC mesophases. It is clear from the exercises followed so far that the CSA values of the Model mesogens are very handy in arriving at the order parameters of the Dimer mesogen from chemical shift alone. For the purpose of comparison, order parameter values obtained from ^{13}C-^{1}H dipolar couplings (two representative measurements) have been incorporated in Figure 10. A good agreement is observed in comparing the order parameters of the phenyl rings of both the mesogens determined from ^{13}C-^{1}H dipolar couplings (two representative measurements) as well as from AIS values. This evidently suggests that the CSA values of the Model mesogen are highly consistent primarily due to the structural resemblance of the core unit in both systems.

The ^{13}C NMR studies of Model mesogen and Dimer mesogens leading to CSA as well as ^{13}C-^{1}H dipolar couplings will be valuable for investigating the order parameters of main chain liquid crystalline polymers in which phenyl benzoate is part of the core unit. It is often difficult to determine the CSA values for main chain liquid crystalline polymers in a solid state due to inherent line broadening. In such a scenario, making use of CSA values determined from the model mesogens as demonstrated in the present study would be of great convenience to determine the order parameters of such polymeric systems in the liquid crystalline phase.

Conclusions

A Model mesogen and its Dimer in which the core unit was constructed with phenyl benzoate were examined by ^{13}C NMR spectroscopy in the liquid crystalline phase and determined the orientational order parameters. The existence of SmA and SmC mesophases for the Dimer was established by HOPM, DSC, and XRD techniques. Significantly a large difference between measured layer spacing (d) and molecular length (L) of Dimer mesogen ($0.5 < d/L < 1$) in the SmA phase was attributed to the intercalation of a few carbons of terminal dodecyloxy chains into neighbouring layers. ^{13}C CPTOSS experiment was carried out for the Model mesogen in the solid phase and using CPPI, the assignment of different carbons of the core unit was accomplished. The CSA values of the Model mesogen were determined by SUPER experiment in the solid phase while 2D SLF NMR was employed for extracting ^{13}C-^{1}H dipolar couplings in the liquid crystalline phase. Thus the order parameters of phenyl rings of the core unit of both the mesogens were accomplished using CSA values along with AIS and also from ^{13}C-^{1}H dipolar couplings. The main order parameters (S_{zz}) for the Model mesogen were in the range of 0.54–0.82 in the nematic and SmC phases. For the Dimer mesogen, the S_{zz} values in SmA and SmC mesophases were in the span of 0.64–0.82. A good agreement was noted between the order parameters calculated from ^{13}C-^{1}H dipolar couplings as well as AIS values and was attributed to the structural similarity of the core unit present in the Model and Dimer mesogens.

Experimental Section

Instrumental Details

^{1}H and ^{13}C NMR spectra of the samples were run on a 400 MHz Bruker Avance -III HD NMR spectrometer at room temperature using $CDCl_3$/DMSO-d_6 as solvent and tetramethylsilane (TMS) as an internal reference. The resonance frequencies of ^{1}H and ^{13}C were 400.23 MHz and 100.64 MHz respectively. Optical polarizing micrographs were taken using a Carl Zeiss axiocam MRC5 polarizing microscope equipped with a Linkam THMS heating stage with TMS 94 temperature programmer. The samples were placed between 12 mm glass coverslips and transferred to the heating stage and heated at a programmed heating rate. The photomicrographs were taken using an imager A2 M digital camera. Differential scanning calorimetry traces were recorded using a DSC Q 200 instrument at a heating rate of 10 °C for a minute in a nitrogen atmosphere. The samples were subjected to two heating and two cooling cycles. The data obtained from the second heating and cooling cycle was considered for discussion. DSC Q 200 is calibrated for the heat flow enthalpy and temperature. For transition temperature, the calibration is done using the indium metal with melting temperature at 156.6 °C and heat of fusion 27.71 J/g. The heat flow into the calibration material or the difference of temperature between the calibration material and a reference is monitored and continuously recorded. Powder XRD studies of the un-oriented samples filled in Lindemann capillary of a diameter of 1 mm, (Hampton Research, Aliso Viejo, CA, USA) were carried out using PANalytical instrument (DY 1042-Empyrean) operating with a line focused Ni-filtered Cu–Kα (λ = 1.54 Å) beam and a linear detector (PIXcel 3D). The sample temperature was controlled with a precision of 0.1 °C using a heater and a temperature controller (Linkam).[69]

Solid State NMR Measurements

The solid-state ^{13}C NMR experiments were conducted for the Model mesogen using a Bruker AV-III 500 MHz spectrometer (^{1}H: 500.17 MHz, ^{13}C: 125.79 MHz) equipped with both a 4 mm triple resonance MAS probe for spinning conditions and a 5 mm double resonance probe with a horizontal solenoid coil for static conditions. For the Dimer mesogen, Bruker AV-III HD 400 MHz spectrometer (^{1}H: 400.07 MHz, ^{13}C: 100.61 MHz) with a 5 mm double resonance probe featuring a horizontal solenoid coil was used.

2D SUPER pulse sequence[25] was employed to generate ^{13}C CSA powder patterns for the Model mesogen at room temperature. This experiment was conducted at a spinning speed (ω_r) of 4.61 kHz. The resulting spectrum provides a correlation between the anisotropic ^{13}C CSA powder patterns (F1 dimension) and their associated ^{13}C isotropic chemical shifts (F2 dimension). After a ramp-CP contact time of $\tau = 4$ ms, we recoupled the ^{13}C CSA using a pair of two rotor-synchronized ^{13}C 2π pulses, corresponding to a radio frequency (rf) strength of $\omega_C = 12.12^*\omega_r = 55.9$ kHz during the t_1 period. We applied ^{1}H continuous wave (CW) decoupling with an rf field strength of 119 kHz during the CSA recoupling period. The recoupled ^{13}C CSA powder patterns in the F1 dimension were scaled to 0.155. To obtain sideband-free spectra, we employed TOSS (total suppression of spinning sidebands) and included a γ-integral delay of 1 ms before acquisition. We utilized 32 t_1 increments, each with 64 scans, and a repetition time of 4 s. The data were acquired using the States-TPPI mode and processed accordingly.

We utilized a CPTOSS (cross-polarization total suppression of spinning sidebands) scheme[57] with a linear ramp ranging from 50% to 100% on the ^{1}H channel (CP Period) to acquire a ^{13}C spectrum of the Model mesogen. This experiment was conducted at a spinning speed of 5 kHz, with a contact time of 4 ms, 748 scans, and a recycle delay of 5 s. For the CPPI (cross-polarization phase inversion) spectral editing scheme,[60] the pulse length of the phase inversion pulse was optimized to 45 μs. In both 1D and 2D experiments, the ^{1}H 90° and ^{13}C 180° pulse lengths were 4 μs and 8 μs, respectively. We employed a TPPM-15[70] decoupling sequence with an rf strength of 83 kHz during the acquisition of carbon signals. ^{13}C chemical shifts were externally referenced to the carbonyl signal of glycine at 176.03 ppm.

For static ^{13}C NMR measurements in the liquid crystalline phase, finely powdered samples at room temperature were packed into 4 mm Zirconia rotors with BN_3 caps. These rotor assemblies were then inserted into 5 mm glass tubes and placed within a 5 mm horizontal solenoid coil. To align the samples in the magnetic field, the sample is heated to the isotropic phase and slowly cooled to the liquid crystalline phase and allowed to stabilize for 15 min before starting the experiment. We utilized a CP sequence (linear ramp from 50% to 100% on the ^{1}H channel) to acquire 1D ^{13}C NMR spectra for both Model/Dimer mesogens in their respective mesophases. The experimental parameters included a ^{1}H 90° pulse length of 4 μs/5 μs, a contact time of 3 ms/3 ms, 256/256 scans, and a recycle delay of 5 s/8 s. For measuring the ^{13}C-^{1}H dipolar couplings of the mesogens in the mesophase, we employed the SAMPI-4 2D SLF pulse sequence.[55] Specifically for Model/Dimer mesogens, we used the following parameters: ^{1}H 90° pulse width of 4 μs/5 μs, contact time τ of 3 ms/3 ms, 148/128 t1 points, 20/64 scans, and relaxation delays of 12 s/10 s (to prevent sample heating). In both 1D and 2D measurements, the SPINAL-64[71] decoupling sequence was employed with an rf strength of 30 kHz

during the acquisition of carbon signals. The resulting 2D data matrix was double Fourier transformed, featuring 4096 and 512 points in the F2 and F1 dimensions, respectively. The ^{13}C chemical shifts were externally referenced to chloroform resonance at 77.2 ppm.

Supporting Information Summary

It contains materials, synthetic procedures, and schemes of Model and Dimer mesogens; ^{13}C CPTOSS and CPPI spectra of Model mesogen.

Acknowledgements

The authors extend gratitude to Dr. K. J. Sreeram, Director of CSIR-CLRI, and acknowledge the financial support provided by the Council of Scientific and Industrial Research (CSIR), New Delhi, in the form of a Senior Research Fellowship for G. P. and Y. S. K. R. Additionally, K. V. R. is thankful to CSIR, India, for granting the Emeritus Scientist position (no.21(1018)/15/EMR-II). CSIR-CLRI Communication No. 1918.

Conflict of Interests

The authors declare no conflict of interest.

Data Availability Statement

The data that support the findings of this study are available in the supplementary material of this article.

Keywords: Liquid crystals · Mesogen · Dimer · ^{13}C NMR · Order parameters · CSA · ^{13}C-^{1}H dipolar couplings

[1] J. I. Jin, S. Antoun, C. Ober, R. W. Lenz, *Br. Polym. J.* **1980**, *12*, 132–146.
[2] K. M. Herbert, H. E. Fowler, J. M. McCracken, K. R. Schlafmann, J. A. Koch, T. J. White, *Nat. Rev. Mater.* **2022**, *7*, 23–38.
[3] C. T. Imrie, G. R. Luckhurst, in *The Handbook of Liquid Crystals, 8 Vol. Set Vol. 7* (Eds: J. W. Goodby, P. J. Collings, T. Kato, C. Tschierske, H. Gleeson, P. Raynes), Wiley-VCH Verlag & Co. KGaA, Weinheim, Germany **2014**, pp. 137–210.
[4] A. Greiner, H.-W. Schmidt, in *The Handbook of Liquid Crystals, 8 Vol. Set Vol. 7* (Eds: J. W. Goodby, P. J. Collings, T. Kato, C. Tschierske, H. Gleeson, P. Raynes), Wiley-VCH Verlag & Co. KGaA, Weinheim, Germany **2014**, pp. 1–28.
[5] D. Pavel, D. Hibbs, R. Shanks, *Adv. Res. Polym. Sci.* **2006**, 65–84.
[6] C. T. Imrie, P. A. Henderson, *Chem. Soc. Rev.* **2007**, *36*, 2096–2124.
[7] G. R. Luckhurst, *Ber. Bunsenge. Phys. Chem.* **1993**, *97*, 1169–1187.
[8] C. T. Imrie, P. A. Henderson, *Curr. Opin. Colloid Interface Sci.* **2002**, *7*, 298–311.
[9] G. R. Luckhurst, *Macromol. Symp.* **1995**, *96*, 1–26.
[10] D. Dunmur, *Crystals* **2022**, *12*, 309.
[11] R. J. Mandle, *Soft Matter* **2016**, *12*, 7883–7901.
[12] D. Chen, J. H. Porada, J. B. Hooper, A. Klittnick, Y. Shen, M. R. Tuchband, E. Korbloèa, D. Bedrov, D. M. Walba, M. A. Glaser, J. E. Maclennan, N. A. Clark, *Proc. Natl. Acad. Sci. USA* **2013**, *110*, 15931–15936.
[13] G. R. Luckhurst, *Tutorial 1, 23 Rd International Liquid Crystal Conference (ILCC 2010)*, July11–16, Kraków, Poland 2010.
[14] R. Y. Dong, Ed, *Nuclear Magnetic Resonance Spectroscopy of Liquid Crystals*, World Scientific Publishing Co., Singapore **2010**.
[15] K. Müller, M. Geppi, *Solid State NMR: Principles, Methods, and Applications*, Wiley-VCH GmbH, Weinheim, Germany **2021**.
[16] N. P. Lobo, K. V. Ramanathan, T. Narasimhaswamy, *Magn. Reson. Chem.* **2020**, *58*, 988–1009.
[17] N. P. Lobo, B. B. Das, T. Narasimhaswamy, K. V. Ramanathan, *RSC Adv.* **2014**, *4*, 33383–33390.
[18] M. K. Reddy, E. Varathan, N. P. Lobo, B. B. Das, T. Narasimhaswamy, K. V. Ramanathan, *J. Phys. Chem. C* **2014**, *118*, 15044–15053.
[19] J. Xu, K. Fodor-Csorba, R. Y. Dong, *J. Phys. Chem. A* **2005**, *109*, 1998–2005.
[20] M. K. Reddy, P. J. Shalini, N. P. Lobo, A. Roy, T. Narasimhaswamy, *Phys. Chem. Chem. Phys.* **2023**, *25*, 14158–14169.
[21] B. Veeraprakash, G. Pratap, N. P. Lobo, K. V. Ramanathan, T. Narasimhaswamy, *ChemPhysChem* **2023**, *24*, e202300074.
[22] B. M. Fung, *Prog. Nucl. Magn. Reson. Spectrosc.* **2002**, *41*, 171–186.
[23] T. Nakai, H. Fujimori, D. Kuwahara, S. Miyajima, *J. Phys. Chem. B* **1999**, *103*, 417–425.
[24] S. Caldarelli, M. Hong, L. Emsley, A. Pines, *J. Phys. Chem.* **1996**, *100*, 18696–18701.
[25] S. F. Liu, J. D. Mao, K. Schmidt-Rohr, *J. Magn. Reson.* **2002**, *155*, 15–28.
[26] B. Heinrich, D. Guillon, *Mol. Cryst. Liq. Cryst. Sci. Technol. Sect. A* **1995**, *268*, 21–43.
[27] M. E. Neubert, T. T. Blair, Y. Dixon-Polverine, M. Tsai, C.-C. Tsai, *Mol. Cryst. Liq. Cryst.* **1990**, *182*, 269–286.
[28] A. C. Griffin, T. R. Britt, *J. Am. Chem. Soc.* **1981**, *103*, 4957–4959.
[29] A. C. Griffin, T. R. Britt, *Mol. Cryst. Liq. Cryst.* **1983**, *92*, 149–155.
[30] J.-I. Jin, H.-T. Oh, J.-H. Park, *J. Chem. Soc. Perkin Trans. 2* **1986**, 343–347.
[31] J.-I. Jin, E.-J. Choi, S.-C. Ryu, R. W. Lenz, *Polym. J.* **1986**, *18*, 63–70.
[32] C. K. Ober, J.-I. Jin, Q. Zhou, R. W. Lenz, in *Advances in Polymer Science, Vol. 59* (Ed: N. A. Platé), Springer-Verlag, Berlin, Heidelberg **1984**, pp. 103–146.
[33] T. Kato, J. Uchida, T. Ichikawa, B. Soberats, *Polym. J.* **2018**, *50*, 149–166.
[34] H. Finkelmann, A. H. Price, C. Hilsum, E. P. Raynes, *Philos. Trans. R. Soc. London Ser. A* **1997**, *309*, 105–114.
[35] T. S. Hebner, K. Korner, C. N. Bowman, K. Bhattacharya, T. J. White, *Sci. Adv.* **2023**, *9*, eade1320.
[36] G. E. Bauman, J. D. Hoang, M. F. Toney, T. J. White, *ACS Macro Lett.* **2023**, *12*, 248–254.
[37] I. Dierking, *Textures of Liquid Crystals*, Wiley-VCH Verlag & Co. KGaA, Weinheim, Germany **2003**.
[38] R. Pratibha, N. V. Madhusudana, *J. Phys. II* **1992**, *2*, 383–400.
[39] I. Nishiyama, T. Yamamoto, J. Yamamoto, J. W. Goodby, H. Yokoyama, *J. Mater. Chem.* **2003**, *13*, 1868–1876.
[40] V. F. A. Ye, N. H. Tinh, V. Laux, N. Isaert, *Ferroelectrics* **1996**, *179*, 9–24.
[41] T. Niori, S. Adachi, J. Watanabe, *Liq. Cryst.* **1995**, *19*, 139–148.
[42] B. Veeraprakash, N. P. Lobo, T. Narasimhaswamy, A. B. Mandal, *Phys. Chem. Chem. Phys.* **2015**, *17*, 19936–19947.
[43] Y. Yamamura, T. Murakoshi, S. Iwagaki, N. Osiecka, H. Saitoh, M. Hishida, Z. Galewski, M. Massalska-Arodź, K. Saito, *Phys. Chem. Chem. Phys.* **2017**, *19*, 19434–19441.
[44] Y. Yamamura, T. Murakoshi, M. Hishida, K. Saito, *Phys. Chem. Chem. Phys.* **2017**, *19*, 25518–25526.
[45] Y. Yamamura, R. Tsuchiya, S. Fujimura, M. Hishida, K. Saito, *J. Phys. Chem. B* **2017**, *121*, 1438–1447.
[46] Y. Yamamura, M. Ito, K. Sugai, H. Noda, Z. Galewski, K. Saito, *Soft Matter* **2023**, *19*, 7245–7254.
[47] R. W. Date, C. T. Imrie, G. R. Luckhurst, J. M. Seddon, *Liq. Cryst.* **1992**, *12*, 203–238.
[48] M. K. Reddy, E. Varathan, N. P. Lobo, A. Roy, T. Narasimhaswamy, K. V. Ramanathan, *Langmuir* **2015**, *31*, 10831–10842.
[49] R. Dabrowski, P. Kula, M. Tykarska, J. Przedmojski, W. Piecek, *Mol. Cryst. Liq. Cryst.* **2007**, *475*, 137–149.
[50] S. Diele, S. Tosch, S. Mahnke, D. Demus, *Cryst. Res. Technol.* **1991**, *26*, 809–817.
[51] T.-N. Chan, G.-Y. Yeap, W.-S. Yam, K. Madrak, A. Zep, D. Pociecha, E. Gorecka, *J. Mater. Chem.* **2012**, *22*, 11335–11339.
[52] M. A. Grunwald, J. C. Haenle, K. C. Kreß, R. Forschner, T. Wöhrle, W. Frey, F. Giesselmann, S. Laschat, *Liq. Cryst.* **2018**, *45*, 1626–1636.
[53] C. V. Yelamaggad, G. Shanker, *Tetrahedron* **2008**, *64*, 3760–3771.
[54] C. C. Liao, C. S. Wang, H. S. Sheu, C. K. Lai, *Tetrahedron* **2008**, *64*, 7977–7985.
[55] A. A. Nevzorov, S. J. Opella, *J. Magn. Reson.* **2007**, *185*, 59–70.

[56] H. Neuvonen, K. Neuvonen, P. Pasanen, *J. Org. Chem.* **2004**, *69*, 3794–3800.
[57] W. T. Dixon, *J. Chem. Phys.* **1982**, *77*, 1800.
[58] P. Hodgkinson, *Prog. Nucl. Magn. Reson. Spectrosc.* **2020**, *118–119*, 10–53.
[59] M. Geppi, G. Mollica, S. Borsacchi, C. A. Veracini, *Appl. Spectrosc. Rev.* **2008**, *43*, 202–302.
[60] X. L. Wu, K. W. Zilm, *J. Magn. Reson. Ser. A* **1993**, *102*, 205–213.
[61] K. Eichele, *WSolids1 Ver. 1.21.7*, Universität Tübingen, **2021**.
[62] J. Mason, *Solid State Nucl. Magn. Reson.* **1993**, *2*, 285–288.
[63] T. Narasimhaswamy, *J. Indian Inst. Sci.* **2012**, *90*, 37–53.
[64] Z. H. Gan, *J. Magn. Reson.* **2000**, *143*, 136–143.
[65] C. S. Nagaraja, K. V. Ramanathan, *Liq. Cryst.* **1999**, *26*, 17–21.
[66] N. P. Lobo, M. Prakash, T. Narasimhaswamy, K. V. Ramanathan, *J. Phys. Chem. A* **2012**, *116*, 7508–7515.
[67] J. W. Emsley, J. C. Lindon, *NMR Spectroscopy Using Liquid Crystal Solvents*, Pergamon Press, Oxford **1975**.
[68] B. M. Fung, J. Afzal, T. L. Foss, M. H. Chau, *J. Chem. Phys.* **1986**, *85*, 4808–4814.
[69] S. Radhika, M. Monika, B. K. Sadashiva, A. Roy, *Liq. Cryst.* **2013**, *40*, 1282–1295.
[70] A. E. Bennett, C. M. Rienstra, M. Auger, K. V. Lakshmi, R. G. Griffin, *J. Chem. Phys.* **1995**, *103*, 6951–6958.
[71] B. M. Fung, A. K. Khitrin, K. Ermolaev, *J. Magn. Reson.* **2000**, *142*, 97–101.

Manuscript received: October 13, 2023
Revised manuscript received: August 22, 2024
Accepted manuscript online: August 23, 2024
Version of record online: ■■, ■■

RESEARCH ARTICLE

A model mesogen and its dimer with phenyl benzoate core unit are investigated by ^{13}C NMR spectroscopy in nematic, SmA, and SmC phases to determine the orientational order parameters. Excellent agreement between the order parameters determined from ^{13}C-^{1}H dipolar couplings as well as CSA tensors and ^{13}C chemical shifts is witnessed owing to the structural similarity of the core in both systems.

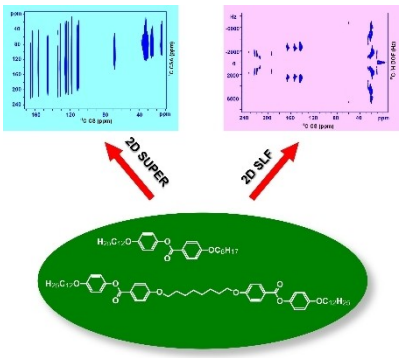

*G. Pratap, Y. S. K. Reddy, N. P. Lobo, K. V. Ramanathan, T. Narasimhaswamy**